Accounts

Circular Dichroism and Absorption Spectroscopy for Three-Membered Ring Compounds Using Symmetry-Adapted Cluster-Configuration Interaction (SAC-CI) Method

Tomoo Miyahara,[1,2] Jun-ya Hasegawa,[1,2,3] and Hiroshi Nakatsuji*[1,2]

[1]Quantum Chemistry Research Institute (QCRI), Kyodai Katsura Venture Plaza, North building 106, 1-36 Goryo-Oohara, Nishikyo-ku, Kyoto 615-8245

[2]Japan Science and Technology Agency, CREST

[3]Department of Synthetic Chemistry and Biological Chemistry, Graduate School of Engineering, Kyoto University, Katsura, Nishikyo-ku, Kyoto 615-8510

Received March 11, 2009; E-mail: h.nakatsuji@qcri.or.jp

The singlet excited states of oxirane and thiirane derivatives, ethylene oxide, (*R*)-methyloxirane, (2*S*,3*S*)-dimethyloxirane, ethylene sulfide, (*R*)-methylthiirane, and (2*S*,3*S*)-dimethylthiirane, were calculated employing the symmetry-adapted cluster (SAC)/SAC-configuration interaction (CI) method. The rotatory strengths of the CD spectra were calculated in the velocity form, which is gauge-origin independent. Both the ultraviolet (UV) spectra and the circular dichroism (CD) spectra obtained with the SAC-CI method were in good agreement with the experimental spectra. In oxirane derivatives, the low-lying excited states were composed of excitations from n and σ orbitals to s, p, and d Rydberg orbitals. The excitation from the σ orbital was especially important in (2*S*,3*S*)-dimethyloxirane because of the steric effect of the methyl substitutions. However, in thiirane derivatives, the excitations to the low-lying excited states were only from the n orbital.

1. Introduction

Circular dichroism (CD)[1] is a powerful spectroscopic technique for determining the absolute configuration of chiral molecules. Many theoretical approaches toward understanding experimental CD spectra have recently been reported, including the ab initio self-consistent field (SCF) method,[2,3] multireference configuration interaction (MRCI) method,[4–6] time-dependent density functional theory (TDDFT),[7–12] and coupled-cluster (CC) level theories.[13–21]

The electronic spectra of methyl-substituted oxirane and thiirane have been the subjects of many experimental[2–4,22] and theoretical studies.[2–21] Furthermore, CD spectroscopy can provide additional information about the excited states of substituted oxirane and thiirane derivatives. These three-membered rings are small molecules with chiral properties and rigid structures, and the previous theoretical studies have shed light on the electronic structures of the ground and excited states of methyloxirane, *trans*-2,3-dimethyloxirane, methylthiirane, and *trans*-2,3-dimethylthiirane. Peyerimhoff and co-workers[4–6] reported that the theoretical CD spectra obtained using the MRCI method reproduced the shape of the experimental UV and CD spectra, but the calculated peak positions were lower for the oxirane derivatives and higher for the thiirane derivatives than those of the experimental spectra. This was similar to the theoretical CD spectra obtained by the TDDFT method.[9,11,12,14] On the other hand, the CC method[15,18] gave, in general, a better agreement with the experimental CD spectra in both the shapes and the peak positions.

In particular, Crawford and co-workers[15–18] reported systematic theoretical studies of optical rotatory dispersion and electric CD spectra using CC linear-response theory (LRT).[23] The CD spectra of methyloxirane and methylthiirane were in good agreement with the experimental spectra, for both the excitation energies and the rotatory strength.[18] They extended similar calculations to many other molecules.

Recently, the symmetry-adapted cluster-configuration interaction (SAC-CI) theory[24–33] has provided the CD spectra of dichalcogen derivatives[28,29] and uridine,[30] in which the gauge-variant method was used. However, a gauge-invariant method is necessary for calculation on larger molecules, in contrast to these small molecules. Herein, we calculate the vacuum ultraviolet (VUV) and CD spectra of the methyl-substituted oxirane and thiirane derivatives employing the SAC-CI theory using a gauge-invariant method. The SAC-CI method has been well established since 1978[24,25,27,33] as a reliable and useful method for studying ground and excited states, ionized states, and electron-attached states. The CCLRT is essentially the same theory as the SAC-CI theory.

Published on the web October 8, 2009; doi:10.1246/bcsj.82.1215

Table 1. The Gauge-Origin Dependence of Rotatory Strength of (*R*)-Methyloxirane by Length and Velocity Forms

State	EE /eV	Osc /au	Rotatory strength[a] ($z = 0.0$ Å)		Rotatory strength[a] ($z = 100.0$ Å)		Exptl[b]	
			Length $/10^{-40}$ cgs	Velocity $/10^{-40}$ cgs	Length $/10^{-40}$ cgs	Velocity $/10^{-40}$ cgs	EE /eV	Rotatory strength $/10^{-40}$ cgs
1^1A	7.02	0.009	−10.253	−10.974	3.835	−10.974	7.08	−12.5
2^1A	7.42	0.010	−0.896	−1.016	−2.348	−1.016		
3^1A	7.48	0.016	5.355	5.238	−32.025	5.238		
4^1A	7.67	0.011	1.898	2.108	18.044	2.108	7.70	+5.9
5^1A	7.85	0.004	6.644	7.742	0.824	7.742		
6^1A	8.39	0.005	−0.826	−1.809	2.745	−1.809		
7^1A	8.44	0.029	−9.971	−8.976	56.506	−8.976	8.35	−4.1
8^1A	8.52	0.002	−4.698	−4.954	−23.345	−4.954		
9^1A	8.64	0.006	1.210	1.349	3.684	1.349		

a) 1 esu cm erg G^{-1} in cgs units $\approx 3.336 \times 10^{-15}$ C M J T^{-1} in SI units. b) From Reference 22.

2. Rotatory Strength

The rotatory strength (R_{0a}) of the CD spectra can be calculated using the length-gauge expression, which is the imaginary part of the scalar product of the electric and the magnetic transition moments between the ground state (Ψ_0) and the excited state (Ψ_a).[34]

$$R_{0a} = \mathrm{Im}\{\langle\Psi_0|\hat{\mu}|\Psi_a\rangle\langle\Psi_a|\hat{m}|\Psi_0\rangle\} \quad (1)$$

where $\hat{\mu}$ is the electric dipole moment operator and $\hat{m}$ is the magnetic dipole moment operator. The electric transition dipole moment is gauge-origin independent if the ground and excited state wave functions are orthogonal to each other. However, the magnetic transition dipole moment is gauge-origin dependent. For this reason, we use a different expression for the CD rotatory strength as given by,

$$R_{0a} = \mathrm{Im}\left\{\frac{\langle\Psi_0|\nabla|\Psi_a\rangle\langle\Psi_a|\hat{m}|\Psi_0\rangle}{E_a - E_0}\right\} \quad (2)$$

which is in the velocity form and gauge-origin independent.[35] Equation 1 is readily transformed to eq 2 using the Hypervirial theorem:[36]

$$\langle\Psi_a|\nabla|\Psi_0\rangle = (E_a - E_0)\langle\Psi_a|\hat{\mu}|\Psi_0\rangle \quad (3)$$

In the present work, we give the results in both the length and velocity forms in the tables, and in only the velocity forms in the figures.

3. Computational Details

The ground state geometries of the oxirane and thiirane derivatives were optimized with Gaussian03[37] using the density-functional theory (DFT)[38–41] with B3LYP functional[42,43] for the 6-31G(d,p) basis set.[44,45] For the SAC/SAC-CI calculations, the basis functions employed were cc-pVTZ[46,47] sets plus double Rydberg functions[48] for the C, O, S, and H atoms of the three-membered rings, and cc-pVDZ[46,47] sets plus double Rydberg functions for the methyl substitutions. Double Rydberg s and p functions were placed at the center of gravity. In the calculations of (*R*)-methyloxirane, we employed cc-pVTZ sets plus double Rydberg functions for the C, O, and H atoms of the three-membered rings, and cc-pVDZ sets for the methyl substitutions to verify the gauge-origin dependence described below.

In the SAC-CI calculations, the core orbitals of the C, O, and S atoms were treated as frozen orbitals, and all singles and selected doubles were included. Perturbation selection[49] was carried out with the threshold sets of 1×10^{-6} hartree for both the SAC and SAC-CI calculations. The SAC-CI CD spectra were convoluted with Gaussian envelopes for description of the Frank–Condon widths and the resolution of the spectrometer. The full width at half maximum (FWHM) of the Gaussian was 0.4 eV. The gauge origin was placed at the center of gravity in all calculations except for those checking for the gauge-origin dependence.

4. Results and Discussion

4.1 Gauge-Origin Dependence. Table 1 shows the gauge-origin dependence of the rotatory strengths of (*R*)-methyloxirane, which are calculated in both length and velocity forms at $z = 0.0$ and 100.0 Å. The gauge origin is at the center of gravity for $z = 0.0$ Å and is 100.0 Å away from the center of gravity for $z = 100.0$ Å. Both results in the velocity and length forms are similar for $z = 0.0$ Å; however, the results in the length form for $z = 100.0$ Å are significantly different from those at $z = 0.0$ Å. Both the signs and absolute values are different, while both results in the velocity form are the same, i.e., gauge-origin independent. If we calculate for small molecules such as the present three-membered rings, we can get reliable results in both length and velocity forms when the gauge origin is at the center of gravity or oxygen atom. However, if we calculate for large molecules such as biological molecules, the results in velocity form are more reliable than those in length form, because we do not know where the gauge origin should be. In the present results, we show the results in only the velocity form in the figures and in both forms in the tables for comparison. Both results are similar because the gauge origin is at the center of gravity.

4.2 Ground States and the Difference between the Oxirane and Thiirane Derivatives. Figure 1 shows the orbital energies of the Hartree–Fock MOs in the HOMO and next-HOMO regions of the oxirane and thiirane derivatives. In oxirane derivatives, the HOMO and next-HOMO are the σ and n(O) orbitals, respectively, and their energies are nearly the

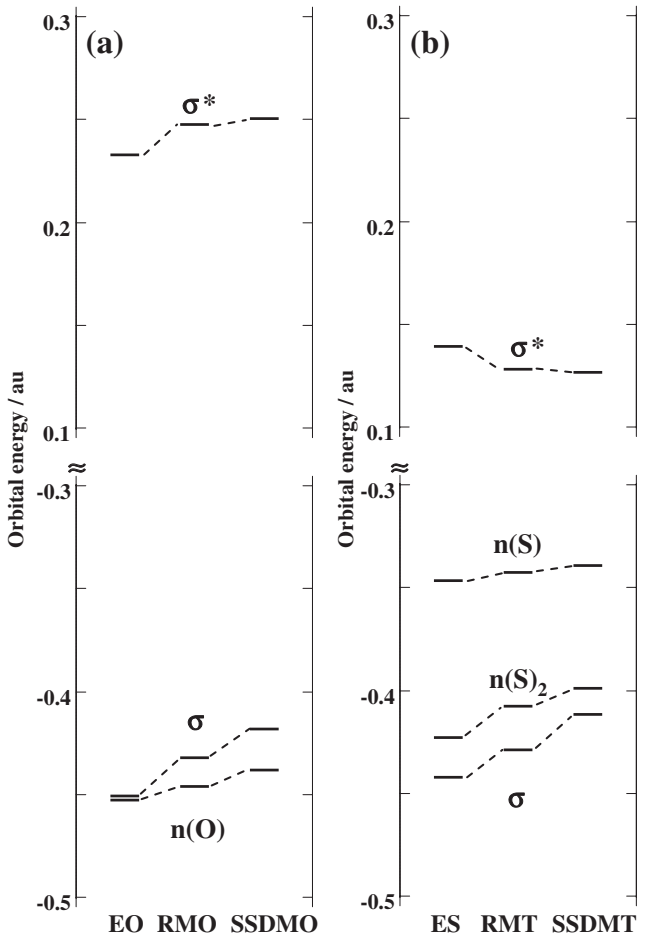

Figure 1. The orbital energies of (a) oxirane and (b) thiirane derivatives. (EO: ethylene oxide, RMO: (*R*)-methyloxirane, SSDMO: (2*S*,3*S*)-dimethyloxirane, ES: ethylene sulfide, RMT: (*R*)-methylthiirane, SSDMT: (2*S*,3*S*)-dimethylthiirane)

same in ethylene oxide (EO). However, the methyl substitutions make the orbital energies of both the σ and n(O) orbitals high, and the energy gap between the HOMO and next-HOMO becomes larger than that of EO (0.002 au), to 0.014 au in (*R*)-methyloxirane (RMO) and to 0.019 au in (2*S*,3*S*)-dimethyloxirane (SSDMO). The methyl substitutions affect the σ orbital more than the n(O) orbital, because the σ orbital has a large amplitude on the carbon atoms of the three-membered rings while the n(O) orbital has the amplitude on the oxygen atom. Although the excitation from the n(O) orbital is lowest, the excitation from the σ orbital is also important in the low-lying excited states. Furthermore, the excited states from the σ orbital are lower in RMO and SSDMO than in EO.

In the thiirane derivatives, the HOMO is the n(S) orbital, which is perpendicular to the plane of the three-membered ring like the n(O) orbital, and its energy is higher than that of the n(O) orbital of the oxirane derivatives by 0.1 au The next-HOMO is the $n(S)_2$, which is on the plane of the three-membered ring. However, the σ orbital has a similar energy to that in the oxirane derivatives. The n(S) and $n(S)_2$ orbitals are less stable than n(O) because they are 4p orbitals. Although the methyl substitution affects the n(S) orbital a little, the σ and $n(S)_2$ orbitals are greatly affected through the carbon atoms of the three-membered ring. The lowest excited state is the excitation from the n(S), and there exist no excited states from the σ orbital below 8.0 eV.

All of the excited states of the oxirane derivatives are excitations to the Rydberg states in the energy range calculated in the present work, because the methyl substitutions make the orbital energies of both the σ and σ^* orbitals higher. However, the first excited states of the thiirane derivatives are the excitation from the σ to the σ^* orbital, and some Rydberg excited states also contain the excitation to the valence orbital (σ^*). The reason for this is shown in Figure 1. The σ^* orbital is stable in the thiirane derivatives more than 0.1 au, compared with that of the oxirane derivatives, although the σ orbital of the thiirane derivatives is less stable than that of the oxirane derivatives by a little. The bond length between the carbon and oxygen is about 1.434 Å in the oxirane derivatives, while that between the carbon and sulfur is about 1.845 Å in the thiirane derivatives. This leads to the unstable nonbonding (n(S)) and the stable antibonding (σ^*) orbitals in the thiirane derivatives. The methyl substitutions make the orbital energy of the σ^* orbital lower in the thiirane derivatives, opposite to that in the oxirane derivatives, because the bond length between the carbon and sulfur is longer in SSDMT than in ES by about 0.016 Å.

4.3 VUV Spectrum of Oxirane (EO). Table 2 shows the excitation energies (EE), oscillator strengths (Osc), second moments $\langle r^2 \rangle$, and the nature of the excitation of the SAC-CI results for EO, which are compared with the experimental spectrum in Figure 2. Fine structure is observed in the first three (I, II, and III) bands in the experimental spectrum. In the absorption spectrum of EO, the first (I) band is assigned to the 1^1B_1 state (7.25 eV), which is the excitation from the n(O) to the 3s Rydberg orbital. Next, there are three states that are the excitations from the n(O) to the 3p Rydberg orbitals. The 2^1B_1 state (7.44 eV) is a shoulder peak of the first (I), the 1^1A_2 state (7.74 eV) has no intensity, and the 1^1A_1 state (7.88 eV) is the second (II) band at 7.89 eV. The 2^1A_1 state is calculated at 8.40 eV and corresponds to the excitation from the σ to the 3s Rydberg orbital. This state is assigned to the shoulder peak of the second (II, 7.89 eV) band. The third (III) band (8.64 eV) is assigned to the 3^1A_1 state (8.70 eV), which is the excitation from the σ to the 3p Rydberg orbital. Vibrational structure is observed in the three (I, II, and III) bands of the experimental spectrum. The fourth (IV) band, with the strongest intensity, is assigned to the 1^1B_2 state (8.85 eV) and 2^1B_2 state (8.95 eV), which are the excitations from the n(O) to the 3d Rydberg orbital, and from the σ to the 3p Rydberg orbital, respectively. The excitation to the valence is slightly mixed in the 2^1B_1 and 3^1A_1 states. Therefore their states have a strong intensity.

There are numerous peaks in the region higher than the fourth (IV) band. We can assign another four (V, VI, VII, and VIII) bands. The fifth (V) band is assigned to the 5^1A_1 state (9.17 eV), which is the excitation from the n(O) to the 4p Rydberg orbital. The sixth (VI) band is assigned to three states (10^1B_1, 7^1A_1, and 11^1B_1 states), which are calculated at 9.64 eV and the excitations from the n(O) to the 4d or 5s Rydberg orbitals. The seventh (VII) band is assigned to the 4^1B_2 state (9.79 eV), and the eighth (VIII) band is assigned to the 5^1B_2 state (9.90 eV). The 4^1B_2 state is the excitation from the n(O) to the 4d Rydberg orbital,

Table 2. Excited States of Ethylene Oxide (Oxirane)

States	EE/eV	Osc/au	$-e\langle r^2\rangle$ /au	Nature of excitation	Exptl[a] EE/eV
X^1A_1	0	0	−41.1		
1^1B_1	7.25	0.013	−82.0	n(O) → 3s	7.24 (I)
2^1B_1	7.44	0.030	−72.2	n(O) → 3p,V	
1^1A_2	7.74	0.000	−90.3	n(O) → 3p,V	
1^1A_1	7.88	0.020	−95.2	n(O) → 3p	7.89 (II)
2^1A_1	8.40	0.011	−82.5	σ → 3s	
2^1A_2	8.44	0.000	−78.6	n(O) → 3d,V	
3^1B_1	8.62	0.003	−133.4	n(O) → 3d	
3^1A_1	8.70	0.035	−76.2	σ → 3p,V	8.64 (III)
1^1B_2	8.85	0.023	−153.1	n(O) → 3d	
4^1B_1	8.91	0.003	−164.7	n(O) → 3d	
2^1B_2	8.95	0.033	−97.5	σ → 3p	8.96 (IV)
4^1A_1	8.98	0.002	−160.9	n(O) → 3d	
5^1B_1	8.99	0.005	−244.4	n(O) → 4s	
6^1B_1	9.02	0.003	−121.3	σ → 3p	
7^1B_1	9.05	0.001	−247.5	n(O) → 4s	
3^1A_2	9.09	0.000	−211.2	n(O) → 4d,V	
5^1A_1	9.17	0.007	−340.5	n(O) → 4p	9.10 (V)
4^1A_2	9.18	0.000	−294.8	n(O) → 4p,V	
8^1B_1	9.52	0.001	−370.2	n(O) → 4p	
5^1A_2	9.57	0.000	−219.2	n(O) → 4d	
6^1A_1	9.58	0.000	−221.1	n(O) → 4d	
3^1B_2	9.60	0.001	−220.6	n(O) → 4d	
9^1B_1	9.61	0.000	−228.7	n(O) → 4d	
6^1A_2	9.61	0.000	−250.8	n(O) → 4d	
10^1B_1	9.64	0.002	−435.3	n(O) → 5s	9.55 (VI)
7^1A_1	9.64	0.001	−230.9	n(O) → 4d	
11^1B_1	9.64	0.002	−244.0	n(O) → 4d	
7^1A_2	9.75	0.000	−515.6	n(O) → 5p	
8^1A_1	9.77	0.005	−495.1	n(O) → 5p	
4^1B_2	9.79	0.020	−260.2	n(O) → 4d	9.68 (VII)
12^1B_1	9.81	0.004	−345.4	n(O) → 4p	
9^1A_1	9.83	0.002	−140.1	σ → 3d	
5^1B_2	9.90	0.022	−125.3	σ → 3d,V	9.87 (VIII)
8^1A_2	9.95	0.000	−246.3	n(O) → 4d,V	
13^1B_1	9.99	0.007	−270.3	n(O) → 4d	

a) From Reference 50.

and the 5^1B_2 state is the excitation from the σ to the 3d Rydberg orbital. Thus the excitations to the 3d, 4s, 4p, and 4d Rydberg orbitals are important in the region higher than the strongest peak (VI). Therefore, to study the peaks in the higher region, the basis set used in the calculations must include higher Rydberg orbitals than those in the present calculations.

4.4 VUV and CD Spectra of (*R*)-Methyloxirane (RMO) and (2*S*,3*S*)-Dimethyloxirane (SSDMO). Table 3 shows the EE, Osc, rotatory strengths in both the length and velocity forms, $\langle r^2\rangle$, and the nature of the excitation for RMO. Figure 3 shows for RMO the experimental VUV and CD spectra compared directly with the SAC-CI results. The SAC-CI absorption peak is shown by a vertical line proportional to the calculated intensity at the calculated excitation energy. There are three principal bands in the experimental CD and VUV spectra. The first one (I) is observed in the range between 7.0 and 7.2 eV and has a rotatory strength with a negative sign. The second (II) is observed in the range between 7.5 and 8.0 eV and has a rotatory strength with a positive sign. The third (III) is a broad band with

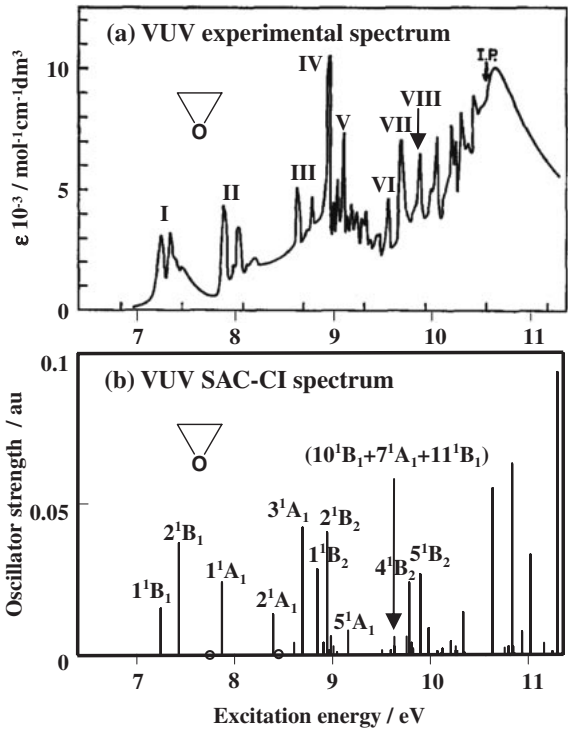

Figure 2. (a) Experimental[50] and (b) SAC-CI VUV spectra of oxirane.

a negative sign in the range between 8.1 and 8.9 eV.

The first (I) band is assigned to the 1^1A state (7.01 eV), which is the excitation from the n(O) orbital to the 3s Rydberg orbital. Vibrational structures are observed in the experimental VUV and CD spectra. The second (II) CD band is composed of one negative (2^1A state at 7.49 eV) and three positive (3, 4, and 5^1A states at 7.56, 7.71, and 7.87 eV) peaks. The 2, 3, and 4^1A states correspond to excitations from the n(O) orbital to the 3p Rydberg orbitals, and the 5^1A state is the excitation from the σ to the 3s Rydberg orbital. The rotatory strength is relatively weak for the 2^1A state compared with those for the 3, 4, and 5^1A states, so that the rotatory strength becomes positive in the range between 7.5 and 8.0 eV. The third (III) band is composed of 10 states, of which the 10^1A state (8.44 eV) is the excitation from the σ to the 3p Rydberg orbital, and has the strongest rotatory and oscillator strengths. The CD spectrum is negative because most strong peaks in the 10 states are negative.

The theoretical SAC-CI results and the experimental results of SSDMO are shown and compared in Table 4 and Figure 4. Four (I, II, III, and IV) bands are observed in the experimental CD spectrum. The first (I) band is positive in the range between 6.9 and 7.1 eV, the second (II) band is negative at 7.35 eV, and the third (III) band is positive in the range between 7.5 and 8.0 eV. A fourth (IV) band is negative in the range between 8.1 and 8.4 eV. The second (II) and third (III) bands appear as one peak in the VUV spectrum.

The first (I) band is assigned to the 1^1B state (7.07 eV), which is the excitation from the n(O) to the 3s Rydberg orbital. Vibrational structures are observed in the experimental VUV and CD spectra as for RMO. The second (II) band corresponds to the 1^1A state (7.39 eV), which is the excitation from the n(O) to the 3p Rydberg orbital. The 2^1B (7.53 eV) and the 2^1A

Table 3. Excited States of (*R*)-Methyloxirane

State	EE /eV	Rotatory strength[a]		Osc /au	$-e\langle r^2\rangle$ /au	Nature of excitation	Exptl[b]	
		Length $/10^{-40}$ cgs	Velocity $/10^{-40}$ cgs				EE /eV	Rotatory strength $/10^{-40}$ cgs
X^1A	0.00	0	0	0	−57.3			
1^1A	7.01	−10.492	−11.446	0.008	−120.4	n(O) → 3s	7.08 (I)	−12.5
2^1A	7.49	−3.95	−4.925	0.015	−117.9	n(O) → 3p		
3^1A	7.56	4.865	4.787	0.013	−132.3	n(O) → 3p		
4^1A	7.71	5.463	6.117	0.013	−145.9	n(O) → 3p	7.70 (II)	+5.9
5^1A	7.87	6.716	7.653	0.006	−120.3	σ → 3s	7.85 (II)	
6^1A	8.29	0.619	0.672	0.003	−204.5	n(O) → 3d		
7^1A	8.34	1.721	1.771	0.002	−197.8	n(O) → 3d		
8^1A	8.36	−3.624	−3.794	0.005	−210.6	n(O) → 3d		
9^1A	8.42	−2.867	−3.647	0.005	−210.7	n(O) → 3d		
10^1A	8.44	−10.302	−9.662	0.024	−145.5	σ → 3p	8.35 (III)	−4.1
11^1A	8.46	−2.006	−2.468	0.010	−145.6	σ → 3p		
12^1A	8.50	−1.319	−1.336	0.001	−267.9	n(O) → 3d		
13^1A	8.51	−0.137	0.169	0.003	−266.0	n(O) → 3d		
14^1A	8.53	0.806	0.520	0.001	−146.1	σ → 3p		
15^1A	8.65	1.431	1.357	0.003	−341.6	n(O) → 4s		

a) 1 esu cm erg G^{-1} in cgs units ≈ 3.336×10^{-15} C M J T^{-1} in SI units. b) From Reference 22.

Table 4. Excited States of (2*S*,3*S*)-Dimethyloxirane

State	EE /eV	Rotatory strength[a]		Osc /au	$-e\langle r^2\rangle$ /au	Nature of excitation	Exptl[b]	
		Length $/10^{-40}$ cgs	Velocity $/10^{-40}$ cgs				EE /eV	Rotatory strength $/10^{-40}$ cgs
X^1A	0	0	0	0	−72.1			
1^1B	7.07	10.496	12.534	0.010	−138.0	n(O) → 3s	6.97 (I)	+9.48
1^1A	7.39	−10.457	−10.368	0.008	−148.7	n(O) → 3p	7.35 (II)	−0.13
2^1B	7.53	5.878	7.086	0.009	−149.3	n(O) → 3p	7.56 (III)	
2^1A	7.66	11.726	11.602	0.004	−137.9	σ → 3s	7.70 (III)	+6.18
3^1A	7.70	0.713	0.513	0.000	−192.1	n(O) → 3p		
3^1B	7.99	−1.309	−0.299	0.005	−148.8	σ → 3p		
4^1B	8.15	−0.024	−0.175	0.011	−231.7	n(O) → 3d		
5^1B	8.22	−10.772	−11.151	0.011	−180.6	σ → 3p	8.15 (IV)	−2.12
4^1A	8.25	9.175	8.749	0.012	−162.5	σ → 3p		
6^1B	8.25	−0.536	−0.315	0.003	−248.0	n(O) → 3d		
7^1B	8.29	−2.523	−2.882	0.002	−239.6	n(O) → 3d	8.31 (IV)	
5^1A	8.33	−2.266	−1.767	0.001	−207.5	n(O) → 3d		
8^1B	8.43	0.752	0.706	0.003	−381.2	n(O) → 4s		
6^1A	8.45	−4.018	−3.474	0.002	−454.5	n(O) → 4p		
9^1B	8.52	3.306	3.730	0.006	−412.9	n(O) → 4p		
7^1A	8.61	1.094	1.082	0.000	−535.6	n(O) → 4p		
8^1A	8.79	−0.948	−1.461	0.001	−229.5	σ → 3d		
10^1B	8.82	−0.460	−0.721	0.000	−206.9	σ → 3d		
9^1A	8.90	−0.801	−0.840	0.001	−255.9	σ → 3d		
11^1B	8.92	2.626	2.363	0.009	−234.6	σ → 3p		
10^1A	8.97	−1.041	−1.025	0.003	−263.2	σ → 3d		

a) 1 esu cm erg G^{-1} in cgs units ≈ 3.336×10^{-15} C M J T^{-1} in SI units. b) From Reference 5.

(7.66 eV) states are assigned to 7.56 and 7.70 eV of the third (III) band, respectively. The 2^1B state is the excitation from the n(O) to the 3p Rydberg orbital, and the 2^1A state is the excitation from the σ to the 3s Rydberg orbital. The excited state from the σ orbital in SSDMO appears in the energy region below that of EO or RMO because the σ orbital is less stable in SSDMO than in EO or RMO. The second (II) band is observed to be very weak because of the first and third bands with a strong positive sign. The fourth (IV) band is composed of eight states. The 4^1B state (8.15 eV) has a strong oscillator strength but its rotatory strength is almost zero. The 5^1B (8.22 eV) and 4^1A (8.25 eV) states, which are excitations from the σ to the 3p

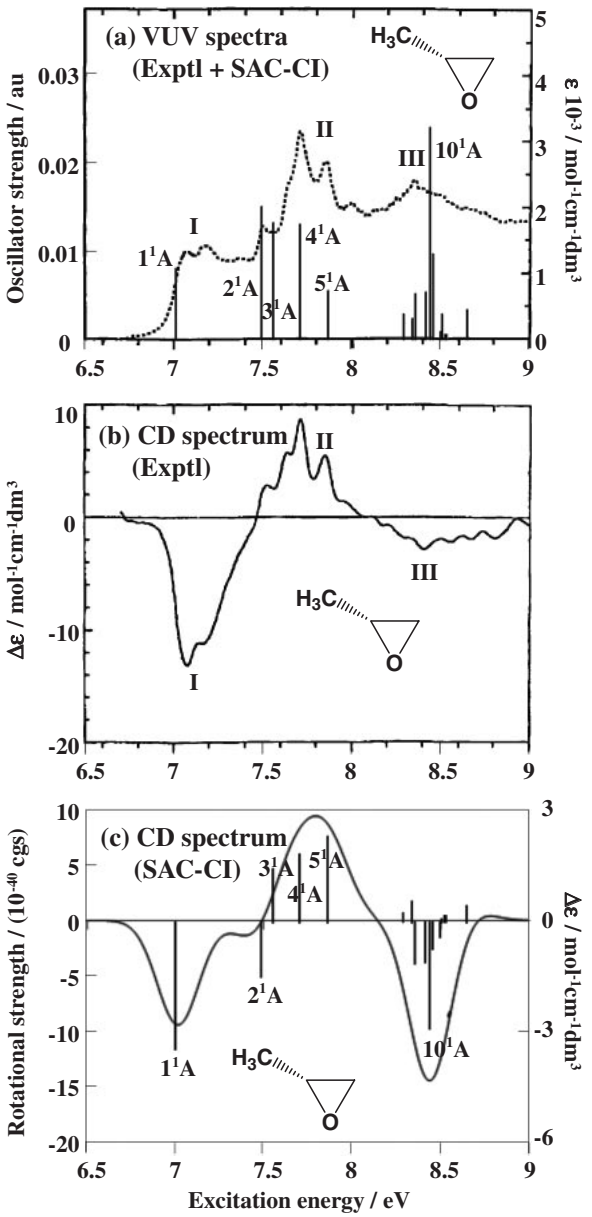

Figure 3. (a) Comparison of the experimental[22] and SAC-CI VUV spectra, (b) the experimental[22] CD spectrum, and (c) the SAC-CI CD spectrum of (*R*)-methyloxirane.

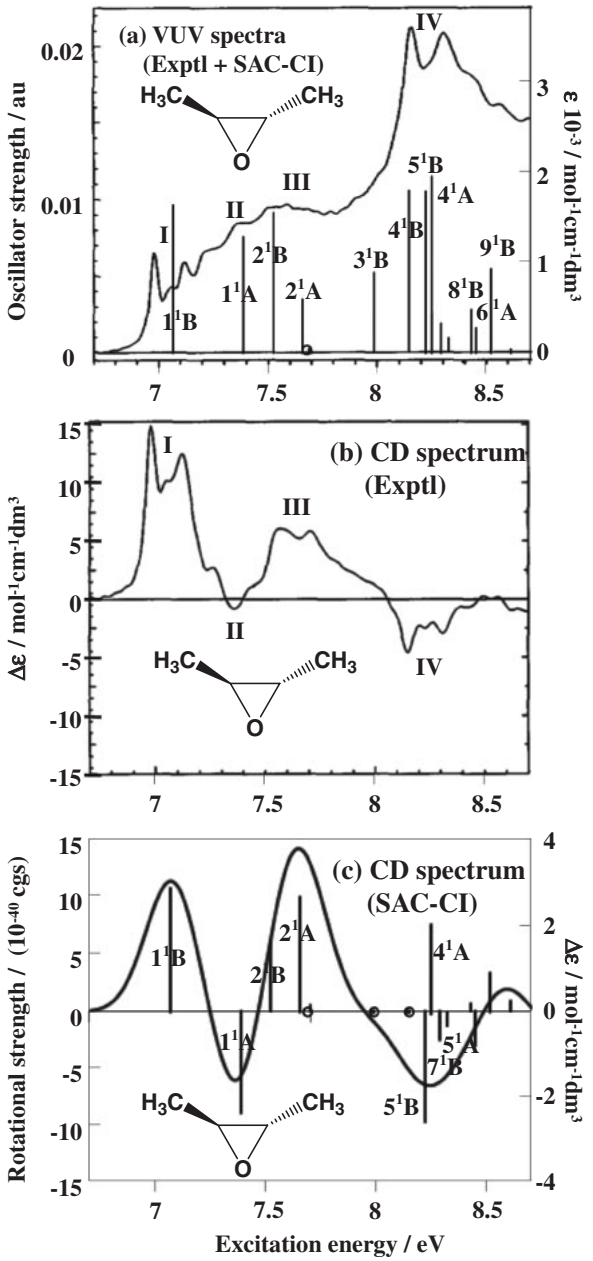

Figure 4. (a) Comparison of the experimental[5] and SAC-CI VUV spectra, (b) the experimental[5] CD spectrum, and (c) the SAC-CI CD spectrum of (2*S*,3*S*)-dimethyloxirane.

Rydberg orbitals, have strong oscillator and rotatory strengths and corresponds to the peak at 8.15 eV of the experimental CD spectrum. However, the fourth (IV) band of the CD spectrum is not strong compared with the VUV spectrum, because the 5^1B is negative and the 4^1A is positive in rotatory strength. The 7^1B (8.29 eV) and the 5^1A (8.33 eV) states are excitations from the n(O) to the 3d Rydberg orbitals and correspond to the peak at 8.3 eV of the experimental CD spectrum. Three states of the 8^1B (8.43 eV), 6^1A (8.45 eV), and 9^1B (8.52 eV) states correspond the shoulder peaks of the fourth (IV) band. In RMO and SSDMO, the valence orbital are not mixed with the Rydberg orbital, which is different from the case of EO.

4.5 Comparison of Oxirane (EO) and Substituted Methyloxiranes (RMO and SSDMO). Figure 5 compares the excitation energies of EO, RMO, and SSDMO. The excitation energies from the n(O) to the 3s Rydberg orbitals are 7.25 eV in EO, 7.01 eV in RMO, and 7.07 eV in SSDMO. These energies are shifted lower by 0.2 eV by methyl substitutions.

In Figure 5, there are three peaks that correspond to the excitations from the n(O) to the 3p Rydberg orbitals. Two states are not affected by the methyl substitutions, but the 1^1A_1 state (7.88 eV) in EO corresponds to the 3^1A state (7.56 eV) in RMO, and to the 1^1A state (7.39 eV) in SSDMO. The excitation energies are again lowered by methyl substitutions, because the node of the p Rydberg orbital is horizontal on the three-membered ring plane in EO, but is not horizontal because of the methyl substitutions in RMO and SSDMO.

The excitation from the σ to the 3s Rydberg state is the 2^1A_1 state (8.40 eV) in EO, the 5^1A state (7.87 eV) in RMO, and the

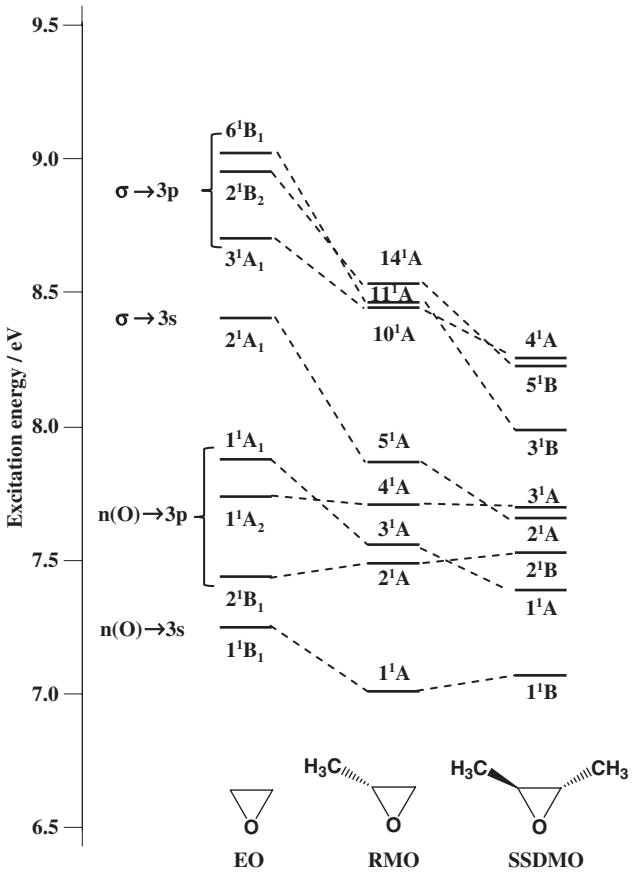

Figure 5. The excitation energies of oxirane derivatives.

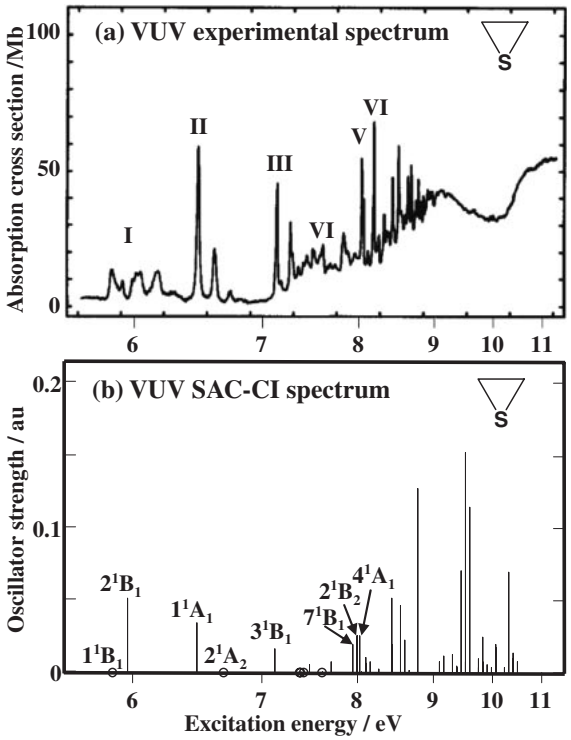

Figure 6. (a) Experimental[51] and (b) SAC-CI VUV spectra of thiirane.

2^1A state (7.66 eV) in SSDMO. The methyl substitutions affect the σ orbital more significantly than the n(O) orbital, as shown in Figure 1. This is because the σ orbital is on the plane of the three-membered ring in EO, but inclines from the plane in both RMO and SSDMO. Therefore, the energy of the σ orbital is highest in SSDMO and lowest in EO.

There are three peaks that correspond to the excitations from the σ to the 3p Rydberg orbitals. The 3^1A_1 state (8.70 eV), the 2^1B_2 state (8.95 eV), and the 6^1B_1 state (9.02 eV) in EO correspond to the 10^1A state (8.44 eV), the 14^1A state (8.53 eV), and the 11^1A state (8.46 eV) in RMO, and the 4^1A state (8.25 eV), the 5^1B state (8.22 eV), and the 3^1B state (7.99 eV) in SSDMO. These states are shifted because of the excitation from the σ orbital. In particular, the 3^1B state (7.99 eV) in SSDMO is shifted by 1.0 eV, because it corresponds to the excitation from the σ to the p Rydberg orbital with an inclination of the node.

The 1^1B_2 state (8.85 eV), the excitation from the n(O) to the 3d Rydberg orbital in EO, corresponds to the 4^1B state (8.15 eV) in SSDMO, however, there is no state with a strong intensity corresponding to the excitation to the 3d Rydberg orbital in RMO.

4.6 VUV Spectra of Thiirane (Ethylene Sulfide: ES). Figure 6 and Table 5 show the theoretical and experimental results for ES. The low-lying excited states are the excitation from n(S) and the lowest excited state from the σ orbital is the 9^1A_1 state (8.54 eV). The first excited state is the 1^1A_2 state (4.94 eV) with no intensity that corresponds to the excitation from the n(S) to the σ^* orbital. This is very different from EO, because the molecular orbital energy of the σ^* of ES is lower than that of EO by 0.09 au. However, this state is not observed in either ES or EO because it is a forbidden transition.

Three (I, II, and III) bands with vibrational structure are observed in the range below 7.5 eV in the experimental VUV spectrum. There are two peaks in the range below 6.0 eV, which is the first (I) band observed in the VUV spectrum. The 1^1B_1 state (5.86 eV), with a very weak intensity, is the excitation from the n(S) to the 4p Rydberg orbital. The 2^1B_1 state (5.96 eV) has a strong intensity, which is the excitation from the n(S) to the 4s Rydberg orbital. These two excited states also mix with the excitation to the σ^* orbital and have a large second moment, because the valence orbitals in the thiirane derivatives are lower than those in the oxirane derivatives.

The 1^1A_1 state (6.45 eV), also with a strong intensity, and the 2^1A_2 state (6.66 eV) are calculated at approximately 6.45 eV. Both states correspond to the excitation from the n(S) to the 4p Rydberg orbitals and the second (II) band observed in the VUV spectrum.

The 3^1B_1 state is calculated at 7.12 eV in the third (III) band, which is the excitation from the n(S) to the 4d Rydberg orbital. States with very small oscillator strength are calculated in the region of the fourth band (VI). Three states (7^1B_1, 2^1B_2, and 4^1A_1 states) with some oscillator strength are calculated at around 8.0 eV corresponding to the fifth band (V). The 2^1B_2 and 4^1A_1 states are the excitation from $n(S)_2$ to the 4p Rydberg and the valence orbitals. However, there is no state with a strong oscillator strength corresponding to the sixth band (VI). Thus, many states beyond 8 eV are calculated, but their assignments are made difficult because of the complicated nature of this spectrum and the lack of basis functions in this calculation.

Table 5. Excited States of Ethylene Sulfide (Thiirane)

States	EE /eV	Osc /au	$-e\langle r^2\rangle$ /au	Nature of excitation	Exptl[a] EE/eV
X^1A_1	0	0	−58.2		
1^1A_2	4.94	0.000	−64.5	n(S) → σ*	
1^1B_1	5.86	0.000	−93.0	n(S) → 4p,V	
2^1B_1	5.96	0.052	−94.2	n(S) → 4s,V	5.84 (I)
1^1A_1	6.45	0.035	−113.9	n(S) → 4p	6.45 (II)
2^1A_2	6.66	0.000	−118.6	n(S) → 4p,V	
3^1B_1	7.12	0.017	−147.6	n(S) → 4d	7.13 (III)
4^1B_1	7.37	0.001	−174.6	n(S) → 4d	
1^1B_2	7.38	0.000	−172.2	n(S) → 4d	
3^1A_2	7.41	0.000	−178.1	n(S) → 4p,V	
5^1B_1	7.45	0.000	−212.7	n(S) → 4s,V	
2^1A_1	7.46	0.007	−188.5	n(S) → 4p	7.50 (IV)
6^1B_1	7.59	0.001	−294.2	n(S) → 5s	
3^1A_1	7.71	0.008	−355.0	n(S) → 5p	
4^1A_2	7.71	0.000	−361.7	n(S) → 5p	
7^1B_1	7.97	0.020	−369.8	n(S) → 5s	
2^1B_2	7.99	0.026	−88.6	$n(S)_2$ → 4p,V	8.04 (V)
4^1A_1	8.02	0.026	−99.0	$n(S)_2$ → 4p,V	
8^1B_1	8.05	0.001	−295.0	n(S) → 4d	
5^1A_2	8.07	0.000	−294.6	n(S) → 4d	
3^1B_2	8.09	0.004	−232.0	n(S) → 4d	
5^1A_1	8.10	0.007	−230.8	n(S) → 4d	
9^1B_1	8.11	0.001	−268.0	n(S) → 4d	
6^1A_2	8.11	0.000	−241.2	n(S) → 4d	
6^1A_1	8.12	0.011	−218.7	n(S) → 4d	
10^1B_1	8.15	0.008	−344.1	n(S) → 4d	
4^1B_2	8.27	0.001	−177.9	n(S) → 4d,V	
7^1A_2	8.28	0.000	−528.2	n(S) → 6p	
7^1A_1	8.29	0.003	−457.8	n(S) → 6p	
11^1B_1	8.30	0.000	−284.4	n(S) → 4d	
8^1A_2	8.34	0.000	−300.8	n(S) → 4d	
5^1B_2	8.36	0.001	−183.2	n(S) → 4d,V	
12^1B_1	8.42	0.000	−372.2	n(S) → 4p	
8^1A_1	8.44	0.020	−310.3	n(S) → 4p	
6^1B_2	8.46	0.052	−91.5	$n(S)_2$ → 4s,V	
9^1A_1	8.54	0.047	−104.0	σ → 4s	
13^1B_1	8.59	0.023	−394.1	n(S) → 5p	
9^1A_2	8.65	0.000	−294.7	n(S) → 4d	
7^1B_2	8.65	0.000	−295.9	n(S) → 4d	
14^1B_1	8.67	0.002	−297.2	n(S) → 4d	
10^1A_2	8.75	0.000	−113.8	$n(S)_2$ → 4p	
10^1A_1	8.82	0.127	−100.6	σ → 4s,V	
11^1A_2	8.95	0.000	−309.4	n(S) → 5d	

a) From Reference 51.

4.7 VUV and CD Spectra of (*R*)-Methylthiirane (RMT) and (2*S*,3*S*)-Dimethylthiirane (SSDMT). Figure 7 shows the experimental and SAC-CI VUV and CD spectra of RMT, and Table 6 shows the details. There are four (I, II, III, and IV) bands up to 7.5 eV in the experimental CD spectrum. The first (I) band is not observed at around 5 eV in the experimental VUV spectrum and has a very small rotatory strength with a negative sign. The second (II) band is observed in the range between 5.64 and 6.34 eV and has a rotatory strength with a negative sign. The third (III) band is observed in the range between 6.34 and 7.00 eV and has maxima at 6.4 eV in the experimental VUV spectrum and at 6.65 eV in the experimental

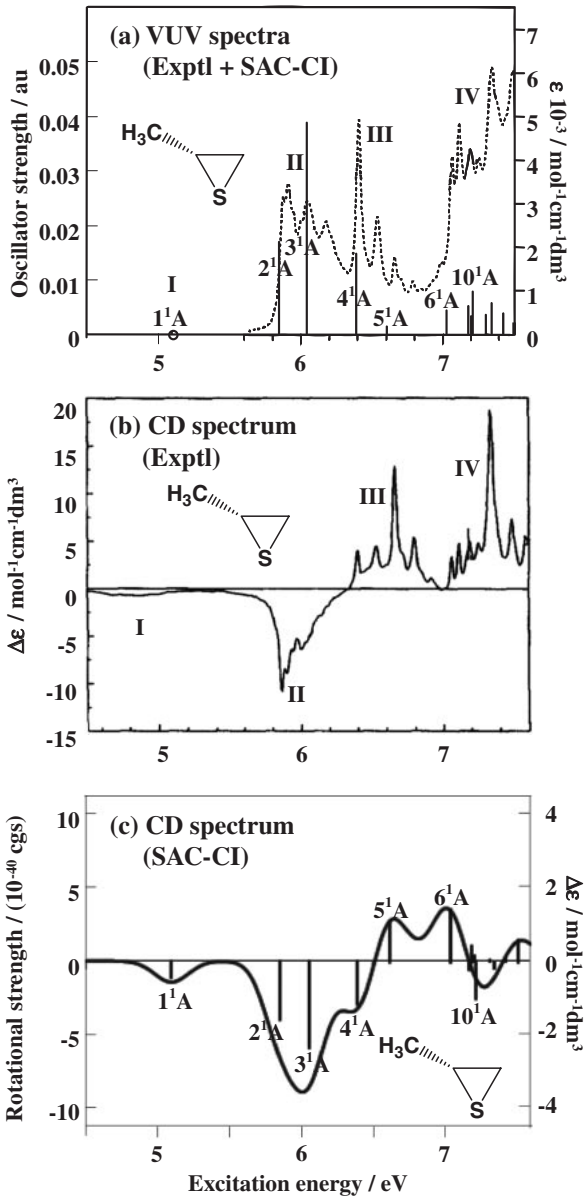

Figure 7. (a) Comparison of the experimental[22] and SAC-CI VUV spectra, (b) the experimental[6] CD spectrum, and (c) the SAC-CI CD spectrum of (*R*)-methylthiirane.

CD spectrum. The fourth (IV) band has a rotatory strength with a positive sign in the range above 7.0 eV.

The first (I) band, with a very small negative intensity, is assigned to the 1^1A state and is calculated at 5.09 eV with very small oscillator and rotatory strengths. In the experimental VUV spectrum, we cannot see a peak in this region. It corresponds to the valence excitation from the n(S) to the σ^* orbital and the first excited state of ES. This type of state is not observed in ES because it is a forbidden transition.

The second (II) band, with a negative intensity in the experimental CD spectrum, is assigned to the 2^1A (5.85 eV) and 3^1A (6.05 eV) states, which are excitations from the n(S) to the 4s and 4p Rydberg orbitals, respectively. The 3^1A state has the strongest oscillator strength in the SAC-CI UV spectrum and the strongest rotatory strength in the SAC-CI CD spectrum.

Table 6. Excited States of (*R*)-Methylthiirane

State	EE /eV	Rotatory strength[a] Length /10^{-40} cgs	Rotatory strength[a] Velocity /10^{-40} cgs	Osc /au	$-e\langle r^2\rangle$ /au	Nature of excitation	Exptl[b] EE /eV	Exptl[b] Rotatory strength /10^{-40} cgs
X^1A	0.00	0	0	0	−75.2			
1^1A	5.09	−1.893	−1.170	0.000	−83.7	n(S) → σ*	4.25/5.25 (I)	−0.2
2^1A	5.85	−1.484	−4.061	0.017	−129.8	n(S) → 4s,V	5.64/6.34 (II)	−9.3
3^1A	6.05	−5.115	−5.935	0.039	−118.8	n(S) → 4p,V		
4^1A	6.39	−2.090	−2.979	0.015	−152.0	n(S) → 4p,V	6.34/7.00 (III)	+6.2
5^1A	6.61	1.960	2.709	0.001	−176.0	n(S) → 4p,V		
6^1A	7.03	4.201	3.395	0.004	−211.1	n(S) → 4d	7.00/7.54 (IV)	+9.7
7^1A	7.16	0.160	−0.600	0.000	−218.6	n(S) → 4d		
8^1A	7.18	0.878	0.946	0.005	−218.4	n(S) → 4d		
9^1A	7.20	0.694	0.397	0.003	−217.1	n(S) → 4d		
10^1A	7.21	−2.162	−2.533	0.008	−218.8	n(S) → 4p		
11^1A	7.30	0.172	0.060	0.004	−351.4	n(S) → 5s		
12^1A	7.34	−0.512	−0.693	0.006	−285.9	n(S) → 4d		
13^1A	7.42	0.266	0.111	0.004	−433.8	n(S) → 5p		
14^1A	7.50	1.425	1.333	0.002	−474.2	n(S) → 5p		

a) 1 esu cm erg G^{-1} in cgs units ≈ 3.336×10^{-15} C M J T^{-1} in SI units. b) From Reference 22.

These states are actually excitations to mixtures of the Rydberg and the σ^* orbitals. Therefore, they have small second moments and strong oscillator strengths.

The third (III) band, with a positive intensity in the experimental CD spectrum, is assigned to the 4^1A (6.39 eV) and 5^1A (6.61 eV) states. These peaks correspond to excitations from the n(S) to 4p Rydberg orbitals. The 4^1A state has a large oscillator strength and is in good agreement with the strongest peak in the 6.34 to 7.00 eV range of the experimental VUV spectrum, while the 5^1A state has a large positive rotatory strength and is in good agreement with the strongest peak in the third (III) band of the experimental CD spectrum. The 4^1A state is in agreement with the peak at 6.4 eV but has a negative sign in the SAC-CI CD spectrum. The sign of the rotatory strength of the 4^1A state may change upon using different basis sets, because this state has a positive sign in the CD calculations using EOM–CCSD, B3LYP, and MRCI with different basis sets from the present calculation.[6,18] However, the rotatory strength of the 4^1A state is also negative in the SAC-CI calculation with aug-cc-pVDZ. Therefore, there is also a possibility that the 4^1A state is assigned to the second (II) band, because the second (II) band is negative in the experimental CD spectrum. A study of the vibrational structure is required to clarify this discrepancy further.

The 6^1A state (7.03 eV) is the lowest peak of the fourth (IV) band and corresponds to the excitation to the 4d Rydberg orbital. There are nine states calculated in the fourth band. These states are the excitations from the n(S) to 4p, 4d, 5s, and 5p Rydberg orbitals, and they require a more extensive basis set for full clarification, because the rotatory strength of the 7^1A state is positive in the length form and negative in the velocity form.

Figure 8 and Table 7 compare the SAC-CI results for SSDMT with the experimental spectra; there are two weak (I and III) and three strong (II, IV, and V) bands up to 7.5 eV in the experimental CD spectrum. The first (I) band is very weak, similar to the case of RMT. The second (II) band is observed in the range between 5.64 and 6.36 eV and has a rotatory strength with a positive sign. The third (III) band with weak positive rotatory strength is observed in the range between 6.51 and 6.64 eV. The fourth (IV) band is observed in the range between 6.65 and 7.23 eV and has a rotatory strength with a negative sign. The fifth (V) band has a rotatory strength with a positive sign in the range above 7.24 eV.

The first (I) band is the 1^1A state calculated at 5.09 eV, which corresponds to the excitation from the n(S) to the σ^* orbital. However, this state is not observed in the experimental VUV spectrum and is also very weak in the experimental CD spectrum compared with other states.

The 1^1B, 2^1B, and 2^1A states are assigned to the second (II) band. The 1^1B state (5.90 eV) is the excitation from the n(S) to the 4s Rydberg orbital. The 2^1B (6.16 eV), 2^1A (6.28 eV), and 3^1A (6.51 eV) states correspond to excitations from the n(S) to the 4p Rydberg orbitals. The 1^1B state has the strongest oscillator strength. However, the 2^1B state has the strongest rotatory strength, and the 1^1B state is the second strongest state in the SAC-CI CD spectrum. Therefore, a study of the vibrational structure may be required to clarify this discrepancy further for SSDMT.

The 3^1A state, with a very weak rotatory strength and no oscillator strength, is assigned to the third (III) band. This band is not observed in the experimental VUV spectrum because this band is in the middle between the second (II) and fourth (IV) strong bands.

There are 12 states in the fourth (IV) and fifth (V) band regions. They correspond to excitations from the n(S) to 4s, 4p, 4d, 5s, and 5p Rydberg orbitals. There is no state with a strong intensity. The lower five states of these states are assigned to the fourth (IV) band, because the sum of the rotatory strengths is negative. The other seven states are assigned to the fifth (V) band. However, a more extensive basis set is needed for full clarification of the fourth and fifth bands.

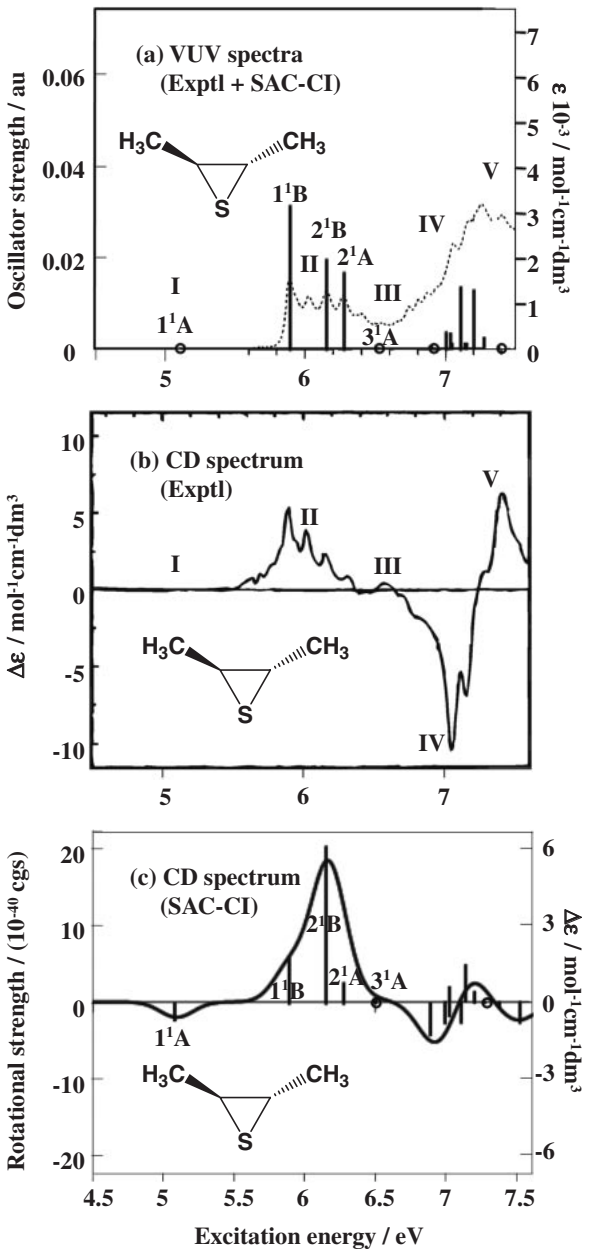

Figure 8. (a) Comparison of the experimental[22] and SAC-CI VUV spectra, (b) the experimental[6] CD spectrum, and (c) the SAC-CI CD spectrum of (2*S*,3*S*)-dimethylthiirane.

In thiirane derivatives, the SAC-CI spectra are in good agreement with the experimental spectra in below 7 eV. However, the shapes of the SAC-CI spectra are different from those of experimental spectra in higher excitation energy region. This may be due to the lack of more diffuse basis sets.

4.8 Comparison of Oxirane and Thiirane Derivatives. In thiirane derivatives, all excited states correspond to excitations from the n(S) below 7.5 eV, because the orbital energy gap between the σ and the n(S) orbitals is greater than 0.07 au. The first weak states correspond to the excitation to the σ^* orbital, because the σ^* orbitals of the thiirane derivatives are much lower than those of the oxirane derivatives. The second band corresponds to the excitation to the 4s (plus 4p) Rydberg orbital with strong oscillator and rotatory strengths, because these excited states are mixed with the σ^* orbital. The third band is the excitation to the 3p Rydberg orbital, and the fourth is the excitation to the 4d Rydberg orbital plus other unidentified states. Thus it is easy to understand the excited states of the thiirane derivatives in the low-lying region.

In oxirane derivatives, the excitation from the σ orbital is important even in the lower region, because the orbital energy gap between the σ and the n(O) orbitals is less than 0.02 au (less than 0.002 au in EO). Therefore, the fifth excited state (2^1A_1, 8.40 eV) is the excitation from the σ orbital in EO, while the lowest excited states corresponding to the excitations from the σ and $n(S)_2$ orbitals are the 35th (9^1A_1, 8.54 eV) and 16th (2^1B_2, 7.99 eV) states in ES, respectively. Therefore, the excited states corresponding to the excitations from the σ and $n(S)_2$ orbitals do not appear in our calculations of RMT and SSDMT, because the excited states are only calculated up to 7.5 eV.

5. Conclusion

In the present work, we have studied both the VUV and CD spectra of oxirane (EO, RMO, and SSDMO) and thiirane (ES, RMT, and SSDMT) derivatives, using the SAC-CI method. The results are in good agreement with the experimental VUV and CD spectra, and the nature of the CD spectra was shown to be very different from that of the VUV spectra. This has clearly deepened the understanding of the electronic structures of the compounds studied. The differences between the SAC-CI results and experimental values are within about 0.1 eV in low-lying excited states. The relative intensities of the SAC-CI spectra are also parallel with those of the experimental spectra.

When the gauge origin was placed at the center of gravity, the two rotatory strengths in the length and velocity forms were nearly identical. However, when the gauge origin was placed away from the center of gravity, the rotatory strengths in the length form were significantly different from those in the velocity form.

In the oxirane derivatives, the lowest band was composed of the excitation from the n(O) to the 3s Rydberg orbitals. In EO, the second band was the excitation from the n(O) to the 3p Rydberg orbital, and the third band was the excitation from the σ to the 3p Rydberg orbital. In RMO, the second band is composed of the excitation of the n(O) to the 3p Rydberg orbital and the σ to the 3s Rydberg orbital, and the third band corresponds to the excitation from the σ to the 3p Rydberg orbital. In SSDMO, the second band is the excitation from the n(O) to the 3p Rydberg orbital, the third band is the excitation from the σ to the 3s Rydberg orbital, and the fourth band is the excitation from the σ to the 3p Rydberg orbital. The excitation energies from the σ orbital are lower in SSDMO than in EO, because the orbital energy of the σ orbital is raised by the methyl substitution.

In the thiirane derivatives, all bands are composed of the excitation from the n(S) orbital, because the orbital energies of the n(S) are destabilized by approximately 0.1 au. The lowest excited state is the excitation to the σ^* orbital at around 5.0 eV. The second band (the first strong band) corresponds to the excitation to the 4s (plus 4p) Rydberg orbital, and the third band (the second strong band) is the excitation to the 4p Rydberg orbital. There is no state displaying an excitation from the σ orbital below 8.0 eV.

Table 7. Excited States of (2*S*,3*S*)-Dimethylthiirane

State	EE /eV	Rotatory strength[a] Length /10^{-40} cgs	Rotatory strength[a] Velocity /10^{-40} cgs	Osc /au	$-e\langle r^2\rangle$ /au	Nature of excitation	Exptl[b] EE /eV	Exptl[b] Rotatory strength /10^{-40} cgs
X^1A	0	0	0	0	−90.5			
1^1A	5.09	−3.198	−2.418	0.000	−97.5	n(S) → σ*	4.73/5.10 (I)	−0.1
1^1B	5.90	2.791	5.784	0.031	−156.5	n(S) → 4s		
2^1B	6.16	17.379	20.320	0.020	−149.1	n(S) → 4p	5.64/6.36 (II)	+5.3
2^1A	6.28	2.574	2.480	0.017	−167.7	n(S) → 4p,V		
3^1A	6.51	1.596	0.323	0.000	−209.3	n(S) → 4p	6.51/6.64 (III)	+0.2
3^1B	6.90	−5.018	−4.503	0.000	−212.9	n(S) → 4d		
4^1B	7.00	−3.633	−2.626	0.003	−242.8	n(S) → 4d		
4^1A	7.04	1.103	2.061	0.001	−241.4	n(S) → 4p	6.65/7.23 (IV)	−7.2
5^1B	7.04	−2.694	−1.955	0.003	−261.3	n(S) → 4d		
5^1A	7.11	−2.574	−2.502	0.013	−270.9	n(S) → 4p		
6^1B	7.15	3.835	4.933	0.001	−297.9	n(S) → 4s		
7^1B	7.21	1.279	1.393	0.013	−398.3	n(S) → 5s		
6^1A	7.28	−0.167	−0.151	0.002	−461.7	n(S) → 5p		
7^1A	7.38	−0.458	−0.677	0.000	−538.8	n(S) → 5p	7.24/7.70 (V)	+4.5
8^1B	7.53	−3.386	−2.492	0.003	−506.1	n(S) → 5s		
8^1A	7.59	−0.189	−0.140	0.000	−332.9	n(S) → 4d		
9^1A	7.63	0.067	0.062	0.002	−326.1	n(S) → 4d		

a) 1 esu cm erg G^{-1} in cgs units ≈ 3.336×10^{-15} C M J T^{-1} in SI units. b) From Reference 22.

We thank Dr. R. Fukuda for the discussion. The computations were performed using Research Center for Computational Science, Okazaki, Japan.

References

1 *Circular Dichroism: Principles and Applications*, 2nd ed., ed. by N. Berova, K. Nakanishi, R. W. Woody, Wiley-VCH, New York, **2000**.
2 D. Cohen, M. Levi, H. Basch, A. Gedanken, *J. Am. Chem. Soc.* **1983**, *105*, 1738.
3 D. Cohen, M. Levi, B. S. Green, R. Arad-Yellin, H. Basch, A. Gedanken, *J. Phys. Chem.* **1983**, *87*, 4585.
4 M. Carnell, S. D. Peyerimhoff, A. Breest, K. H. Gödderz, P. Ochmann, J. Hormes, *Chem. Phys. Lett.* **1991**, *180*, 477.
5 M. Carnell, S. Grimme, S. D. Peyerimhoff, *Chem. Phys.* **1994**, *179*, 385.
6 M. Carnell, S. D. Peyerimhoff, *Chem. Phys.* **1994**, *183*, 37.
7 K. Yabana, G. F. Bertsch, *Phys. Rev. A* **1999**, *60*, 1271.
8 S. Grimme, F. Furche, R. Ahlrichs, *Chem. Phys. Lett.* **2002**, *361*, 321.
9 J. Autschbach, T. Ziegler, S. J. A. van Gisbergen, E. J. Baerends, *J. Chem. Phys.* **2002**, *116*, 6930.
10 J. Autschbach, S. Patchkovskii, T. Ziegler, S. J. A. van Gisbergen, E. J. Baerends, *J. Chem. Phys.* **2002**, *117*, 581.
11 M. Pecul, K. Ruud, T. Helgaker, *Chem. Phys. Lett.* **2004**, *388*, 110.
12 A. C. Neto, F. E. Jorge, *Chirality* **2007**, *19*, 67.
13 K. Ruud, T. Helgaker, *Chem. Phys. Lett.* **2002**, *352*, 533.
14 C. Diedrich, S. Grimme, *J. Phys. Chem. A* **2003**, *107*, 2524.
15 M. C. Tam, N. J. Russ, T. D. Crawford, *J. Chem. Phys.* **2004**, *121*, 3550.
16 T. D. Crawford, *Theor. Chem. Acc.* **2006**, *115*, 227.
17 T. D. Crawford, M. C. Tam, M. L. Abrams, *J. Phys. Chem. A* **2007**, *111*, 12057.
18 T. D. Crawford, M. C. Tam, M. L. Abrams, *Mol. Phys.* **2007**, *105*, 2607.
19 K. Ruud, P. J. Stephens, F. J. Devlin, P. R. Taylor, J. R. Cheeseman, M. J. Frisch, *Chem. Phys. Lett.* **2003**, *373*, 606.
20 J. Kongsted, T. B. Pedersen, M. Strange, A. Osted, A. E. Hansen, K. V. Mikkelsen, F. Pawlowski, P. Jørgensen, C. Hättig, *Chem. Phys. Lett.* **2005**, *401*, 385.
21 J. Kongsted, T. B. Pedersen, L. Jensen, A. E. Hansen, K. V. Mikkelsen, *J. Am. Chem. Soc.* **2006**, *128*, 976.
22 A. Breest, P. Ochmann, F. Pulm, K. H. Gödderz, M. Carnell, J. Hormes, *Mol. Phys.* **1994**, *82*, 539.
23 H. Koch, P. Jørgensen, *J. Chem. Phys.* **1990**, *93*, 3333.
24 H. Nakatsuji, K. Hirao, *J. Chem. Phys.* **1978**, *68*, 2053.
25 H. Nakatsuji, *Chem. Phys. Lett.* **1978**, *59*, 362.
26 H. Nakatsuji, *Chem. Phys. Lett.* **1979**, *67*, 329; H. Nakatsuji, *Chem. Phys. Lett.* **1979**, *67*, 334.
27 H. Nakatsuji, in *Computational Chemistry—Reviews of Current Trends*, ed. by J. Leszczynski, World Scientific, Singapore, **1997**, Vol. 2, pp. 62–124.
28 J. Seino, Y. Honda, M. Hada, H. Nakatsuji, *J. Phys. Chem. A* **2006**, *110*, 10053.
29 Y. Honda, A. Kurihara, M. Hada, H. Nakatsuji, *J. Comput. Chem.* **2008**, *29*, 612.
30 S. Bureekaew, J. Hasegawa, H. Nakatsuji, *Chem. Phys. Lett.* **2006**, *425*, 367.
31 J. Wan, M. Hada, M. Ehara, H. Nakatsuji, *J. Chem. Phys.* **2001**, *114*, 842.
32 H. Nakatsuji, *Bull. Chem. Soc. Jpn.* **2005**, *78*, 1705.
33 J. Hasegawa, H. Nakatsuji, in *Radiation Induced Molecular Phenomena in Nucleic Acids*, ed. by M. K. Shukla, J. Leszczynski, Springer, **2008**, Chap. 4, pp. 93–124.
34 L. Rosenfeld, *Z. Phys.* **1928**, *52*, 161.
35 W. Moffitt, *J. Chem. Phys.* **1956**, *25*, 467.
36 M. Pericou-Cayere, M. Rerat, A. Dargelos, *Chem. Phys.* **1998**, *226*, 297.

37 M. J. Frisch, G. W. Trucks, H. B. Schlegel, G. E. Scuseria, M. A. Robb, J. R. Cheeseman, J. A. Montgomery, Jr., T. Vreven, K. N. Kudin, J. C. Burant, J. M. Millam, S. S. Iyengar, J. Tomasi, V. Barone, B. Mennucci, M. Cossi, G. Scalmani, N. Rega, G. A. Petersson, H. Nakatsuji, M. Hada, M. Ehara, K. Toyota, R. Fukuda, J. Hasegawa, M. Ishida, T. Nakajima, Y. Honda, O. Kitao, H. Nakai, M. Klene, X. Li, J. E. Knox, H. P. Hratchian, J. B. Cross, C. Adamo, J. Jaramillo, R. Gomperts, R. E. Stratmann, O. Yazyev, A. J. Austin, R. Cammi, C. Pomelli, J. W. Ochterski, P. Y. Ayala, K. Morokuma, G. A. Voth, P. Salvador, J. J. Dannenberg, V. G. Zakrzewski, S. Dapprich, A. D. Daniels, M. C. Strain, O. Farkas, D. K. Malick, A. D. Rabuck, K. Raghavachari, J. B. Foresman, J. V. Ortiz, Q. Cui, A. G. Baboul, S. Clifford, J. Cioslowski, B. B. Stefanov, G. Liu, A. Liashenko, P. Piskorz, I. Komaromi, R. L. Martin, D. J. Fox, T. Keith, M. A. Al-Laham, C. Y. Peng, A. Nanayakkara, M. Challacombe, P. M. W. Gill, B. Johnson, W. Chen, M. W. Wong, C. Gonzalez, J. A. Pople, *Gaussian 03, Revision E.05*, Gaussian, Inc., Pittsburgh, PA, **2003**.
38 P. Hohenberg, W. Kohn, *Phys. Rev.* **1964**, *136*, B864.
39 W. Kohn, L. J. Sham, *Phys. Rev.* **1965**, *140*, A1133.
40 *The Challenge of d and f Electrons*, ed. by D. R. Salahub, M. C. Zerner, ACS, Washington, D.C., **1989**.
41 R. G. Parr, W. Yang, *Density-Functional Theory of Atoms and Molecules*, Oxford Univ. Press, Oxford, **1989**.
42 A. D. Becke, *J. Chem. Phys.* **1993**, *98*, 5648.
43 C. Lee, W. Yang, R. G. Parr, *Phys. Rev. B* **1988**, *37*, 785.
44 P. C. Hariharan, J. A. Pople, *Theor. Chim. Acta* **1973**, *28*, 213.
45 M. M. Francl, W. J. Pietro, W. J. Hehre, J. S. Binkley, M. S. Gordon, D. J. DeFrees, J. A. Pople, *J. Chem. Phys.* **1982**, *77*, 3654.
46 T. H. Dunning, Jr., *J. Chem. Phys.* **1989**, *90*, 1007.
47 D. E. Woon, T. H. Dunning, Jr., *J. Chem. Phys.* **1993**, *98*, 1358.
48 T. H. Dunning, P. J. Hay, in *Methods of Electronic Structure Theory, III*, ed. by H. F. Schaefer, Plenum Press, New York, **1977**.
49 H. Nakatsuji, *Chem. Phys.* **1983**, *75*, 425.
50 H. Basch, M. B. Robin, N. A. Kuebler, C. Baker, D. W. Turner, *J. Chem. Phys.* **1969**, *51*, 52.
51 I. Tokue, A. Hiraya, K. Shobatake, *J. Chem. Phys.* **1989**, *91*, 2808.

Tomoo Miyahara has received Ph.D. degree from Kyoto University in 2003. He worked as a post-doctoral researcher at Kyoto University in 2003–2007. He was appointed as a Head of Division at Quantum Chemistry Research Institute since 2007.

Jun-ya Hasegawa has received Ph.D. degree from Kyoto University in 1998. He worked as a Japan Society for the Promotion of Science (JSPS) research fellow in 1997–1999. He was a Post Doc in Prof. B. O. Roos's laboratory at Lund University in Sweden for 1998–1999. He was an assistant professor at Kyoto University in 1999–2008 and appointed as a lecturer since 2008.

Hiroshi Nakatsuji received Ph.D. in 1971 from Kyoto University, where he became a professor in 1990. He was a Visiting Professor of Tokyo Institute of Technology, 1989–1990, a Concurrent Professor of the University of Tokyo, 1996–1998, Trustee, Institute for Fundamental Chemistry, 1997–2000, Director, Fukui Institute for Fundamental Chemistry, Kyoto University 2004–2006. He retired Kyoto University in 2007 and founded Quantum Chemistry Research Institute. He is now a director of QCRI. Since 1993, he is a member of the International Academy of Quantum Molecular Science (France) and since 1994, he is a Board of Director, International Society for Theoretical Chemical Physics. He was awarded The Divisional Award of the Chemical Society of Japan for 1990 and The Chemical Society of Japan Award for 2003.